Breath figure templated self-assembly of porous diblock copolymer films

Aaron E. Saunders,[1] Jasper L. Dickson,[1] Parag S. Shah,[1] Min Young Lee,[2] Kwon Taek Lim,[2] Keith P. Johnston,[1,*] and Brian A. Korgel[1,†]

[1]*Department of Chemical Engineering, Texas Materials Institute, Center for Nano- and Molecular Science and Technology, University of Texas, Austin, Texas 78712, USA*

[2]*Division of Image and Information Engineering, Pukyong National University, Pusan 608-739, Korea*

(Received 19 October 2005; published 28 March 2006)

Porous polyethylene oxide–*b*–polyfluorooctylmethacrylate (PEO-*b*-PFOMA) diblock copolymer films were drop cast onto substrates from Freon (1,1,2-trichlorotrifluoroethane) in a humid atmosphere. The pores in the films exhibit long range hexagonal order in some cases, depending on the PFOMA-to-PEO molecular weight ratio. Films with the best ordered pores were formed with PFOMA-to-PEO ratios of 70 kDa:2kDa. The pores in the polymer films derive from water droplets that condense as Freon evaporates. The polymer stabilizes the water droplets, or "breath figures," which act as an immiscible template that molds the porous film. Increased polymer hydrophobicity reduces the water wettability of the air/Freon interface, which in turn decreases water droplet nucleation, thus influencing the final pore size and spatial order in the polymer films. We describe how water droplet nucleation influences the final pore size and packing order in the polymer films.

DOI: 10.1103/PhysRevE.73.031608 PACS number(s): 68.15.+e, 81.16.−c, 83.80.Uv, 82.70.−y

I. INTRODUCTION

"Breath figures"—an antiquated term that describes the structures made by condensed water vapor on a cold surface—have been studied since the early 20th century by Lord Rayleigh [1,2], Aitken [3], and Baker [4], who reported qualitative differences in water condensation on substrates with various chemical or physical treatments. Many of the fundamental principles of breath figure nucleation and growth kinetics on solid [5–9] and immiscible fluid surfaces [9–12] are now relatively well understood, largely based on the work of Knobler, Beysens, and co-workers in the 1980s and early 1990s. Within the past decade, materials scientists have had relatively good success in utilizing breath figure structures as *self-organized templates* to build ordered macroporous films of polymers and nanocrystals [13–28]. A hydrophobic solution of polymer (or nanocrystals) can be evaporated on a substrate in a humid environment such that evaporative cooling forces water droplet condensation at the air/liquid interface. The colloids stabilize the water droplets and prevent their coalescence. As the solvent continues to evaporate, the droplets grow and self-organize into an array dispersed in the polymer solution. When the solvent evaporates completely, the polymer molds around the water droplets, which eventually evaporate to leave pores in the polymer film.

François and co-workers observed the first ordered porous solid films templated by breath figures: they evaporated the block copolymer polystyrene-*b*-polyparaphenylene from carbon disulfide in a humid atmosphere [13]. Breath figure templating requires that the solute (i.e., the polymer or nanocrystals) prevent water droplet coalescence. This requirement has been met by a wide range of colloidal materials, including polymers with various degrees of branching and chemical composition [13–23], nanocrystals [24–26], and blends of organic and inorganic materials [27,28], which have been cast into ordered porous films by breath figures from various hydrophobic solvents as both two- (2D) [13–16,18–23,29,30] and three dimensional (3D) [17,30] porous films. Three alternative theories about the role of the polymer and mechanism of the breath figure templating process have been suggested [31]. François and co-workers initially proposed that their block copolymers formed a gel at the water-solvent interface due to evaporative cooling, resulting in a semirigid stabilizing polymer layer that would prevent coalescence [13], although they later presented experimental evidence suggesting polymer precipitation occurs at the fluid-fluid interface instead [15]. The sol-gel transition depends strongly on the polymer concentration and morphology, and it has been demonstrated that gel formation is unlikely to occur under many typical conditions used for breath figure formation [15]. Polymer precipitation at the liquid-liquid interface depends strongly on the solubility in the solvent, which may vary widely among different systems—not all polymers used to form porous films from breath figures have low solubility. Researchers have also argued that breath figure templating depends only weakly on the interaction between the polymer and the fluid phases and other stabilizing mechanisms, such as thermocapillary action [17] or the slow draining of a viscous polymer dispersion from between droplets [22] can occur. It is unclear, however, if these alternative mechanisms could stabilize droplets for the duration of the evaporation process (tens to hundreds of seconds). In fact, many polymers are surface active, which would tend to stabilize the condensing water droplets against coalescence. Surface active groups, either polar functional groups on the repeat units of the polymer or polar groups at the chain ends, can induce polymer segregation to the water-solvent interface, thus reducing the fluid/fluid interfacial tension [16,18].

*Corresponding author. Electronic address: johnston@che.utexas.edu

†Corresponding author. Electronic address: korgel@mail.che.utexas.edu

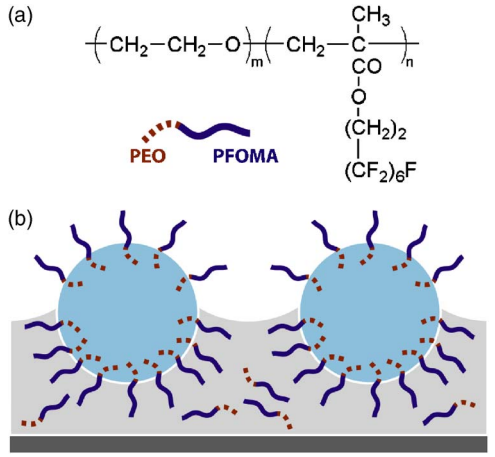

FIG. 1. (Color online) (a) Chemical structure of PEO-*b*-PFOMA. The PEO block has a molecular weight of 2 kDa ($m \approx 45$), with PFOMA blocks varied from 1 to 140 kDa ($n \approx 2$ to 300). (b) The polymer-stabilized water droplets float on a more dense Freon-polymer dispersion. The hydrophilic PEO blocks segregate to the water-Freon interface, while the PFOMA blocks remain in the Freon phase. Surface-tension-driven flow may force some surfactant to the top of the water droplets to decrease the water-air interfacial tension.

In the case of sterically stabilized metal nanocrystals, it was recently found that the capping ligand coating chemistry plays a crucial role in determining the order of pores formed in evaporated nanocrystal films, with interfacial activity being a determining factor [24,25].

Past experimental work has led to a few empirical design rules to manipulate the pore size distribution in the templated films. For example, the size of condensed droplets increases with higher relative humidity [18,23,25,29] due to the larger concentration gradient from the vapor phase to the air/solvent interface which speeds diffusive water transport and condensation. Increased polymer molecular weight has generally given larger pore sizes as well [13,23,29]. Furthermore, since the time available for water droplet growth is directly related to the time for solvent evaporation, varying the dispersion volume placed on the substrate can affect the final pore size [32]. Despite these useful guidelines, there remains a lack of quantitative understanding of droplet nucleation, growth, and stabilization mechanisms in these films, which would be useful for designing interfacially active polymers to control the pore structure. To achieve such an understanding, it would be desirable to design a series of block copolymers with various block lengths to vary the interfacial properties of the system systematically.

Here, we demonstrate that the interfacial activity of an amphiphilic block copolymer polyethylene-*b*-polyfluorooctylmethacrylate (PEO-*b*-PFOMA) [Fig. 1(a)] plays a central role in determining the pore size distribution and order in porous breath figure templated films. Polymers were studied with PEO block lengths of 2 kDa and PFOMA block lengths that ranged from 1 to 140 kDa [33]. Each polymer was dispersed in Freon and evaporated on a substrate under high humidity (90–95 % relative humidity). The hydrophilic-hydrophobic balance of the polymer greatly affected the quality of the porous films and the relative pore size. Measurements of the water/polymer-Freon interfacial tension showed that increasing hydrophilicity (i.e., lower PFOMA molecular weight) lowered the water droplet interfacial tension, consistent with previous measurements of water/CO_2 interfacial tensions of similar polymers [34–36]. This decrease, along with a reduction in the nonequilibrium water/air interfacial tension, correspondingly gave films with decreasing pore size. Films with the highest range of order were formed from polymers with a midrange hydrophobic-hydrophilic balance (2 kDa-*b*-70 kDa PEO-*b*-PFOMA). Polymers that were extremely hydrophilic (e.g., with the PFOMA block below 10 kDa) were relatively insoluble in the evaporating Freon phase and did not stabilize the water droplets sufficiently to give good films. For Freon-soluble polymers that were less hydrophilic (PFOMA molecular weights from 10 to 25 kDa), the final pore size was small with relatively well ordered pores. Very large fluorinated block molecular weights (>140 kDa) significantly inhibited water droplet nucleation and organization. Analysis of the moments of the pore size distribution reveals that droplets grow predominantly by diffusion-limited condensation with little coalescence over time, indicating that changes in the pore sizes obtained from the polymers with PFOMA molecular weights ranging from 10 to 140 kDa do not directly relate to differences in the ability of the surfactant to stabilize the water droplets—all of these polymers prevent coalescence. Rather, the resulting pore size appears to be a function of the droplet nucleation rate, which depends strongly on the surfactant's influence on the water-Freon and water-air interfacial tensions.

II. EXPERIMENTAL METHODS

Poly(ethylene oxide)-block-poly(1*H*,1*H*,2*H*,2*H*-perfluorooctyl methacrylate) [PEO-*b*-PFOMA; Fig. 1(a)] block copolymers were synthesized with PEO block molecular weights of 2 kDa and different PFOMA block molecular weights using previously reported procedures [33]. Polymers with PFOMA block molecular weights of 1, 2, 5, 10, 25, 70, or 140 kDa were studied.

PEO-*b*-PFOMA was dissolved in 1,1,2-trichlorotrifluoroethane (Freon; Aldrich, 99%) at 0.1 wt % concentration. Polymer films were formed by drop casting 10 μl of the 0.1 wt % polymer-Freon solution on oxidized silicon substrates at 25 °C under a stagnant atmosphere with 90–95 % relative humidity. The polymer films were coated with a thin (~2 nm) layer of gold for imaging with a Hitachi S-4500 field emission scanning electron microscope (SEM).

The Freon-water interfacial tension γ_{FW} was measured using pendant-drop tensiometry. A drop of 0.1 wt % polymer-Freon dispersion was introduced into a continuous aqueous phase from an *n*-octyltriethoxysilane surface-modified silica capillary (Western Analytical Products) (180 μm outer diameter, 50 μm inner diameter). A charge-coupled device camera recorded the shape of the drop, which was analyzed using a software package (KSV Instruments Ltd.) that solves the Laplace equation to determine the interfacial tension [37]. The densities of pure water (0.997 g/ml) and Freon

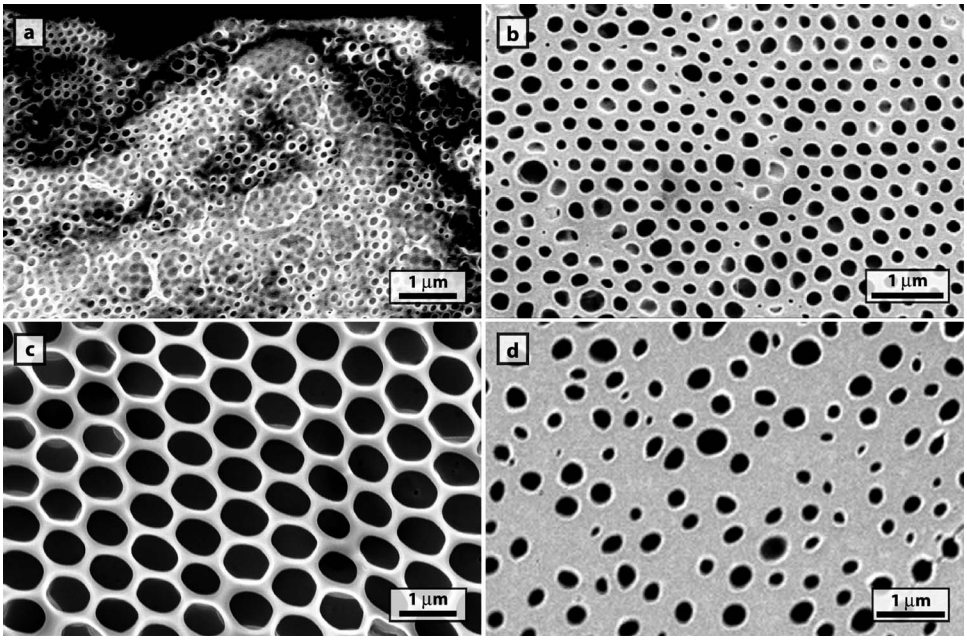

FIG. 2. SEM images of PEO-*b*-PFOMA films cast from 0.1 wt % Freon dispersions under high humidity. The PEO block molecular weight was 2 kDa and the PFOMA block molecular weight was (a) 10, (b) 25, (c) 70, and (d) 140 kDa.

(1.57 g/ml) at 25 °C were used for the interfacial tension calculations.

III. RESULTS

A. Porous PEO-*b*-PFOMA films

Figure 2 shows porous PEO-*b*-PFOMA polymer films drop cast from Freon. The PEO block molecular weight was 2 kDa in each case and the PFOMA block molecular weight was varied from 10 to 140 kDa. Table I summarizes the pore size distributions formed by the different polymers. The pore size and size distribution depended strongly on the PEO-to-PFOMA molecular weight ratio, with the polymer with the PFOMA block weight of 70 kDa giving rise to the most monodisperse and ordered pores (Fig. 3). The porous polymer film in Fig. 3 exhibits long range hexagonal order mediated by grain boundaries. The grain boundaries are most likely the result of the self-organization of "rafts" of close-packed water droplets brought together by lateral capillary forces. Ordered rafts of droplets nucleate and then crystallize with neighboring rafts as the Freon evaporates towards dryness. Lower PFOMA block molecular weights (10 and 25 kDa) [Figs. 2(a) and 2(b)] gave porous films, but with smaller pores and less translational order. PEO-*b*-PFOMA polymers with PFOMA block molecular weights smaller than 10 kDa exhibited poor solubility in Freon and tended to precipitate: pores were never observed in films cast from polymers with the PFOMA block smaller than 10 kDa. The large molecular weight PFOMA block polymer (140 kDa) gave films with polydisperse pores that were separated and poorly ordered [Fig. 2(d)].

B. PEO-*b*-PFOMA interfacial activity and Freon evaporation rates

To better understand the influence of the polymer interfacial activity on the structure of the porous PEO-*b*-PFOMA films, the Freon-water interfacial tension γ_{FW} was measured using a pendent drop tensiometer. Measurements performed on 0.1 wt % PEO-*b*-PFOMA dissolved in the Freon phase

TABLE I. Pore size distribution analysis of PEO-*b*-PFOMA films and interfacial tension measurements.

	Moments and mean radii of pore size distribution						
M_w of PFOMA block (kDa)	Arithmetic mean radius R_1 (nm)	Standard deviation σ (nm)	Cube mean radius R_3 (nm)	Harmonic mean radius R_h (nm)	μ_1	μ_3	γ_{FW}[b] (mN/m)
10	48	15 (33%)	53	43	1.21	0.914	15.1±0.6
25	85	19 (23%)	89	79	1.12	0.952	17.3±0.4
70	354	25 (7%)	356	352	1.01	0.995	22.5±0.7
140	134	65 (24%)	142	125	1.14	0.947	25.6±0.5

[a]The PEO block in each sample had a molecular weight of 2 kDa.
[b]The surface tension of the pure Freon-water system is 28 mN/m.

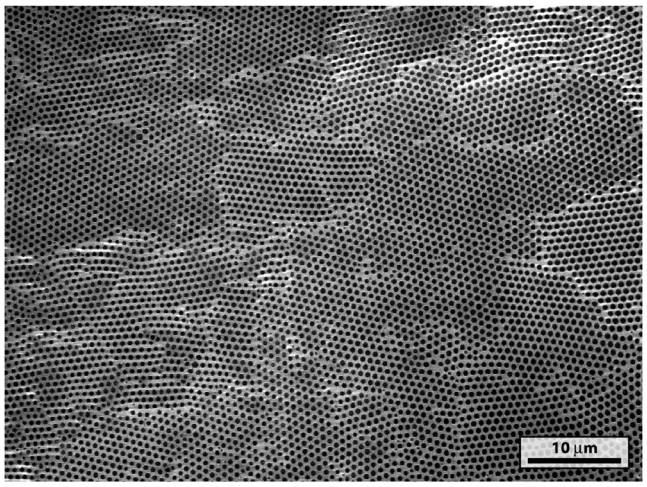

FIG. 3. SEM image of a porous 2–70 kDa PEO-*b*-PFOMA film showing monodisperse pores with long range order.

showed that decreasing PFOMA-to-PEO molecular weight ratios significantly lowered γ_{FW} from its pure Freon/water value of 28 mN/m (Table I). PEO-*b*-PFOMA, with PEO and PFOMA block molecular weights of 2 and 10 kDa, respectively, reduced γ_{FW} to 15 mN/m, which is approximately half the pure Freon/water interfacial tension. PEO-*b*-PFOMA is amphiphilic and decreasing the PFOMA block length makes the copolymer increasingly hydrophilic and more likely to adsorb to the water/Freon interface. Thus, γ_{FW} decreases with decreasing PFOMA molecular weight.

The evaporation rate and temperature drop of 0.1 wt % Freon-polymer solutions were also measured and found to be independent of the PFOMA molecular weight. A clean thermocouple was placed in the evaporating Freon drop to measure the temperature change during evaporation and the rate of temperature rise back to room temperature after the solvent was completely evaporated. The rates and magnitude of the temperature changes were the same for all polymers studied. Evaporation of pure Freon did register a slightly larger temperature drop and faster evaporation rate than the polymer solutions.

IV. DISCUSSION

A. Breath figure formation and growth

As Freon evaporates in the humid atmosphere, evaporative cooling lowers the interface temperature below the dew point temperature forcing water droplets to nucleate. Water then condenses heterogeneously onto the surface of existing water droplets floating at the Freon-air interface until the Freon completely evaporates. Because PEO is hydrophilic and PFOMA is hydrophobic, PEO-*b*-PFOMA tends to orient near the water-Freon interface with PEO exposed to the water phase and PFOMA to the Freon phase, which stabilizes the water droplets and prevents their aggregation and coalescence. Lower PFOMA molecular weight polymers have a greater tendency to partition to the water/Freon interface and stabilize water droplets. Polymers with PFOMA block molecular weight greater than 10 kDa are very soluble in Freon, but PEO-*b*-PFOMA with 2 kDa PEO blocks and PFOMA molecular weights less than 10 kDa do not sufficiently dissolve in Freon to give porous films.

Other researchers have observed a similar trend in breath figure templated polymer films, with good film quality occurring at intermediate polymer molecular weights and deteriorating quality with increased or decreased molecular weight [18,29]. This trend has been attributed by some to the increased dispersion viscosity for high molecular weight polymers, where a high solution viscosity is suggested to provide good droplet stability. While the solution viscosity certainly influences droplet mobility at later stages in the breath figure formation process, severely retarding droplet self-assembly in the case of very high molecular weight [as in Fig. 2(d) for example], changes in viscosity alone cannot explain the differences in observed pore diameter in Fig. 2. If solutions with a low viscosity do not stabilize water droplets very well, there should be a strong tendency for the growing droplets to coalesce and become larger—thus, the lower molecular weight polymers would be expected to cast films with *larger* pore sizes. Instead, Fig. 2 reveals the opposite trend: the pore size increased as the polymer molecular weight increased. So, what factors determine the pore size distribution in the polymer films?

First of all, consider that water droplets may grow via two mechanisms: (1) water vapor can condense onto existing drops (diffusion-limited growth) or (2) neighboring drops can collide and coalesce (coagulative growth). Diffusion-limited growth leads to a narrowing of the size distribution, whereas coagulative growth broadens the distribution. Diffusion-limited and coagulative growth can also occur simultaneously, generally leading to relatively broad size distributions. Previous studies of breath figure growth on fluid surfaces in the absence of stabilizing polymers have demonstrated that water droplets grow primarily through condensation immediately following nucleation [11,12]. As the water droplets increase in size, diffusion-limited growth narrows the droplet size distribution. The water droplets are then attracted to each other by lateral capillary forces, which (in the absence of coalescence) leads to the formation of droplet arrays on the liquid surface. In systems where no stabilizing surfactant is present, neighboring droplets fuse, which quickly destroys order and causes the size distribution to broaden significantly. The pore size distribution in the films in Figs. 2(a)–2(c) are all relatively narrow, indicating that water droplet aggregation is not significant and that PEO-*b*-PFOMA stabilizes the water droplets over the time required for Freon to evaporate.

A quantitative analysis of the moments of the pore size distribution $\mu_1 = R_3/R_h$ and $\mu_3 = R_1/R_3$ reveals more clearly the relative contributions of diffusion-limited and coagulation-driven water droplet growth to the formation of the pores. $R_1 = (\Sigma R_i)/N$ is the arithmetic mean radius, $R_3 = \sqrt[3]{(\Sigma R_i^3)/N}$ is the cube mean radius, and $R_h = N/(\Sigma 1/R_i)$ is the harmonic mean radius, where R_i is the radius of pore i, and N is the total number of pores. For systems in which condensation and aggregation may both occur simultaneously, Pich, Friedlander, and Lai determined that values of $\mu_1 > 1.25$ and $\mu_3 < 0.905$ indicate that diffusion-limited condensation controls growth [38]. Values of the mean radii and

the moments of the pore size distributions for the films in Fig. 2 are reported in Table I. In each film, μ_1 and μ_3 indicate that water droplets grow primarily by diffusion-limited condensation. These results confirm that PEO-*b*-PFOMA polymers, with FOMA-block molecular weights between 10 and 140 kDa, stabilize the water droplets against aggregation until the continuous phase becomes sufficiently viscous to reduce droplet mobility.

The ability of various PFOMA-*b*-PEO surfactants to stabilize water droplets against coalescence has also been observed in water/CO_2 emulsions [34–36]. In those studies, polymers with less than 20 wt % EO in the block copolymer—similar to those studied here—favored the nonaqueous CO_2 phase and stabilized water/carbon dioxide (rather than carbon dioxide/water) emulsions. Surfactant adsorption at the water/CO_2 interface was sufficient to prevent coalescence in some cases for more than 1 day [34,36]. The very weak interactions between solvated PFOMA chains [35] that encourage steric stabilization of water droplets in low viscosity CO_2 also occur in Freon.

B. Relationship between pore surface coverage and nucleation

If aggregative growth does not occur in any of the films, what gives rise to the difference in pore size and size distribution in the various films? The pores in the polymer film in Fig. 2(c) exhibit hexagonal close packing and ordering, and the films in Figs. 2(a) and 2(b) are nearly close packed. The pores in the film in Fig. 2(d) are poorly ordered. As described below, the difference in pore size and packing order appears to relate to differences in water droplet nucleation rates, which depend sensitively on the hydrophobicity of the polymer.

Water is less dense than Freon, so water droplets float at the Freon-air surface and eventually give rise to a two-dimensional layer of close-packed pores [as observed in Figs. 2(a)–2(c)]. One can relate the pore size to the relative nucleation rate in the following manner. Consider that a hexagonal close-packed layer of disks has a (2D) surface coverage θ_{pores}, of 91%. Therefore, by approximating the pores in all three films in Figs. 2(a)–2(c) as monodisperse and close packed, the 2D surface coverage of the pores in each film is *approximately* the same—91%—the only difference between the films is then the total number of pores per area. Assuming the droplets to be confined to two dimensions and do not overlap during growth, as is the case in Figs. 2(a)–2(c), θ_{pores} is the same in each film even though the pore size and number of nuclei may vary. θ_{pores} can be written explicitly in terms of the nucleation rate at time t' (in units of number/cm^2 s) $J_n(t')$, and the area occupied by each pore n (nucleated at time t') at time t, $\pi R_n(t,t')^2$ [39]:

$$\theta_{pores} = \int_0^t J_n(t')\,\pi R_n(t,t')^2 d\tau. \tag{1}$$

The pore sizes in Figs. 2(a)–2(c) are relatively monodisperse, such that $\pi R_n(t,t')^2$ is approximately equal throughout each individual film. In order to have a monodisperse collection of pores, the nucleation event must occur at a reasonably discrete time early in the evaporation process, making t' approximately the same for each pore in each film. Using the prime and double prime to denote the two different polymer films, Eq. (1) can be rewritten as

$$\theta'_{pores} = \int_0^{t_1} J'_n(t')\,\pi R'_n(t,t')^2 d\tau \approx \theta''_{pores} = \int_0^{t_2} J''_n(t')\,\pi R''_n(t,t')^2 d\tau \tag{2}$$

Since the evaporation rates of the polymer films were approximately equal regardless of the PFOMA molecular weight, $t_1 \approx t_2$. In order for one film to have a smaller final pore size, *it must have a higher nucleation rate*. In other words, considering that the water droplets grow by diffusion-limited growth, the pore size difference in the polymer films in Figs. 2(a)–2(c) must result from different water droplet nucleation rates early in the Freon evaporation process.

C. Breath figure nucleation rate

The rate of water droplet nucleation depends on the hydrophobicity of the air/Freon interface. The nucleation flux J(number/cm^2 s) can be written as a function of an activation energy $\Delta\Omega$, which is the work required to form the nucleus at the air/Freon interface, such that [40,41]

$$J = J_0 \exp\left(\frac{-\Delta\Omega}{kT}\right), \tag{3}$$

k is Boltzmann's constant, and T is the temperature. $\Delta\Omega$ can be estimated using a "capillary approximation" (neglecting line tension effects) by taking a spherical cap as the shape of the heterogeneously nucleated water droplet [41]:

$$\Delta\Omega = \frac{16\pi\gamma_{W\text{-}air}^3 f(\theta_{FW})}{3(\Delta P)^2} \tag{4}$$

ΔP is the difference in water partial pressure in the gas phase and vapor pressure at the liquid surface, and $\gamma_{W\text{-}air}$ is the water-air surface tension. $f(\theta_{FW})$ is a geometrical factor derived from the spherical cap shape of the water droplet and is a function of the Freon-water contact angle θ_{FW} [8,40,41]:

$$f(\theta_{FW}) = \frac{2 - 3\cos\theta_{FW} + \cos^3\theta_{FW}}{4}. \tag{5}$$

The nucleation rate depends much more strongly on the exponential than the preexponential factor and hence [40]

$$J \propto \exp\left(-\frac{16\pi\gamma_{W\text{-}air}^3 f(\theta_{FW})}{3(\Delta P)^2 kT}\right). \tag{6}$$

From Eq. (6), it is evident that the nucleation rate *depends on the water wettability of the Freon liquid surface* [5,40]. The nucleation rate increases as the contact angle at the water-Freon-air interface decreases, i.e., as the interactions between the water droplets and the Freon-polymer solution become more energetically favorable, and $\gamma_{W\text{-}air}$ decreases. This behavior has in fact been observed experimentally for breath figure formation (i.e., water droplet condensation) on solid surfaces of increasing hydrophobicity by Zhao and Beysens,

who observed a decrease in the droplet nucleation rate as the substrate became more hydrophobic [8]. The nucleation rate in Eq. (6) also depends on the water vapor supersaturation (ΔP). Our findings that the temperature drop and evaporation kinetics are independent of the PFOMA molecular weight suggest that the supersaturation does not measurably vary with changes in surfactant, and hence the nucleation rate is primarily a function of the surfactant-mediated surface tensions.

The Freon/water contact angle θ_{FW} relates to γ_{FW} through Young's equation:

$$\gamma_{F\text{-}air} - \gamma_{FW} = \gamma_{W\text{-}air} \cos \theta_{FW}, \tag{7}$$

where $\gamma_{F\text{-}air}$ is the Freon-air surface tension and $\gamma_{W\text{-}air}$ is the water-air surface tension. The decrease in the measured values of γ_{FW} with a decrease in PFOMA molecular weight will lower θ_{FW}, according to Eq. (7). The polymer does not significantly affect $\gamma_{F\text{-}air}$; since the surface tension of pure Freon is already quite low and there is only a small driving force for the polymer to arrange itself at the Freon-air interface. In addition to modifying the Freon-water interfacial tension (Table I) the presence of surfactant may also modify $\gamma_{W\text{-}air}$. There is a large surface tension gradient between the top of the water droplet ($\gamma_{W\text{-}air}$=72 mN/m for pure water) and the Freon/water interface. Even though the polymers are water insoluble, Marangoni flow may drive polymer onto the top of the condensing water droplets [see Fig. 1(b)] to decrease the water-air surface tension [42]. A decrease in $\gamma_{W\text{-}air}$ produced by coverage of the upper part of the droplets with a monolayer of surfactant will further cause a decrease in θ_{FW}.

Whereas γ_{FW} has been measured explicitly at equilibrium for a known concentration of surfactant in Freon, the determination of $\gamma_{W\text{-}air}$ is more complex. Pendant drop tensiometry may not be used to measure the range of lowering of $\gamma_{W\text{-}air}$ of interest, since the surfactant is extremely insoluble in water [33]. Furthermore, the value of $\gamma_{W\text{-}air}$ for a monolayer of surfactant on top of the nucleating droplets is a nonequilibrium value influenced by Marangoni flow. However, $\gamma_{W\text{-}air}$ may be estimated qualitatively from the observed lowering of a similar property, the water-CO_2 interfacial tension γ_{WC}. At 35 °C, the equilibrium values of γ_{WC} decreased from 10 mN/m for a surfactant with 10 wt. % EO to less than 1 mN/m for 20 wt. % EO, for 7 kDa PFOMA and 2 kDa PEO [34–36]. These decreases are relatively large, and it is very likely that the nonequilibrium value of $\gamma_{W\text{-}air}$ will also decrease significantly relative to a clean water/air interface, favoring more rapid nucleation. Furthermore, the relative values of $\gamma_{W\text{-}air}$ resulting from the presence of the polymer will be higher for larger PFOMA molecular weight polymers, similar to the trend observed for these surfactants at the water-Freon interface in Table I, and at the water/CO_2 interface as discussed in Refs. [34,36]. Thus, decreases in PFOMA molecular weight should decrease both θ_{FW} (from reductions in both γ_{FW} and $\gamma_{W\text{-}air}$) and $\gamma_{W\text{-}air}$, leading to faster nucleation according to Eq. (6). This prediction of Eq. (6) is exactly what is observed in Fig. 2 in that the number of droplets per area increases with a decrease in PFOMA molecular weight, as a consequence of a decrease in θ_{FW} and in $\gamma_{W\text{-}air}$.

V. CONCLUSIONS

The water droplet size formed during breath figure templating of polymer films depends strongly on the interfacial activity of the polymer molecules. The primary factor controlling the pore size and size distribution in the case of the PEO-*b*-PFOMA polymers studied here appears to be the relative water droplet nucleation rates. The PEO-*b*-PFOMA polymer lowers θ_{FW} from reductions in γ_{FW} and $\gamma_{W\text{-}air}$, making the Freon/air interface more wettable. With a decrease in the PFOMA block length, or likewise an increase in surfactant hydrophilicity, water droplet nucleation rates increased consistent with theory, on the basis of reductions in γ_{FW} and $\gamma_{W\text{-}air}$, and consequently θ_{FW}. After a burst of water droplet nucleation, heterogeneous condensation—that is, condensation on existing water droplets at the Freon interface—takes over and nucleation ceases. Water molecules may diffuse directly from the gas phase to the droplet surface or adsorb molecularly on the Freon surface and diffuse across the surface [6]; either mechanism leads to a sharp water droplet size distribution regardless of the initial distribution [43]. Taking into account that the Freon evaporation rate and temperature drop due to evaporative cooling do not depend significantly on the PFOMA block molecular weight, *the total amount of water condensed on the evaporating films must be approximately the same*. The difference in pore size therefore relates to the differences in nucleation density—higher nucleation densities provide more diffusion "sinks" to absorb the condensing water and result in smaller final droplet size. When the PFOMA block is too large relative to the PEO block, water droplet nucleation is largely prohibited due to the poor wettability of the Freon/air interface. As a result, very few pores form in these polymer films, as observed in Fig. 2(d).

The hydrophobic-hydrophilic balance of the polymer is important in stabilizing water droplets and preventing their coalescence, however, the polymer must also have good solubility in the hydrophobic solvent. Tuning the hydrophobic-hydrophilic balance of block copolymers appears to be a promising way to produce porous films with different pore sizes and spacing.

ACKNOWLEDGMENTS

This work is supported in part by the STC Program of the National Science Foundation under Agreement No. CHE-9876674, the Department of Energy, and the Robert A. Welch Foundation. A.E.S. gratefully acknowledges support from the Nanotechnology Foundation of Texas.

[1] L. Rayleigh, Nature (London) **86**, 416 (1911).
[2] L. Rayleigh, Nature (London) **90**, 436 (1912).
[3] J. Aitken, Nature (London) **86**, 516 (1911).
[4] T. J. Baker, Philos. Mag. **44**, 752 (1922).
[5] D. Beysens and C. M. Knobler, Phys. Rev. Lett. **57**, 1433 (1986).
[6] J. L. Viovy, D. Beysens, and C. M. Knobler, Phys. Rev. A **37**, 4965 (1988).
[7] D. Beysens, C. M. Knobler, and H. Schaffar, Phys. Rev. B **41**, 9814 (1990).
[8] H. Zhao and D. Beysens, Langmuir **11**, 627 (1995).
[9] D. Beysens, Atmos. Res. **39**, 215 (1995).
[10] C. M. Knobler, and D. Beysens, Europhys. Lett. **6**, 707 (1988).
[11] A. Steyer, P. Guenoun, D. Beysens, and C. M. Knobler, Phys. Rev. B **42**, 1086 (1990).
[12] A. Steyer, P. Guenoun, and D. Beysens, Phys. Rev. E **48**, 428 (1993).
[13] G. Widawski, M. Rawiso, and B. Francois, Nature (London) **369**, 387 (1994).
[14] O. Pitois and B. Francois, Colloid Polym. Sci. **277**, 574 (1999).
[15] O. Pitois and B. Francois, Eur. Phys. J. B **8**, 225 (1999).
[16] O. Karthaus *et al.*, Langmuir **16**, 6071 (2000).
[17] M. Srinivasarao *et al.*, Science **292**, 79 (2001).
[18] X. Zhao *et al.*, J. Appl. Polym. Sci. **90**, 1846 (2003).
[19] L. Cui *et al.*, Polymer **45**, 8139 (2004).
[20] B. Erdogan *et al.*, J. Am. Chem. Soc. **126**, 3678 (2004).
[21] L. Song *et al.*, Adv. Mater. (Weinheim, Ger.) **16**, 115 (2004).
[22] M. Haupt *et al.*, J. Appl. Phys. **96**, 3065 (2004).
[23] Y. Xu, B. Zhu, and Y. Xu, Polymer **46**, 713 (2005).
[24] P. S. Shah *et al.*, Adv. Mater. (Weinheim, Ger.) **15**, 971 (2003).
[25] A. E. Saunders *et al.*, Nano Lett. **4**, 1943 (2004).
[26] J. Li *et al.*, Langmuir **21**, 2017 (2005).
[27] A. Boeker *et al.*, Nat. Mater. **3**, 302 (2004).
[28] B. C. Englert *et al.*, Chem.-Eur. J. **11**, 995 (2005).
[29] J. Peng *et al.*, Polymer **45**, 447 (2004).
[30] M. S. Park and J. K. Kim, Langmuir **20**, 5347 (2004).
[31] Water droplets can also be stabilized through the adsorption of solid particles, such as nanocrystals [see Refs. [24,25] and Y. Lin, Science **299**, 226 (2003), for example], at the solvent-water interface—comparable to "Pickering," emulsions [B. P. Pinks, Science **7**, 21 (2002)]. In this case there is not a significant reduction in the interfacial tension; instead, the nanocrystals reduce the area of the energetically unfavorable solvent-water interface. The energy needed to remove a single nanocrystal from the interface can be several times the thermal energy kT. The removal of many nanocrystals from the liquid-liquid interface—which is needed for droplet coalescence to occur—thus constitutes a significant energetic barrier against water droplet aggregation.
[32] T. Nishikawa *et al.*, Mater. Sci. Eng., C **C10**, 141 (1999).
[33] K. T. Lim *et al.*, Polymer **43**, 7043 (2002).
[34] P. Psathas, Ph.D. thesis, The University of Texas at Austin, 2001.
[35] J. L. Dickson *et al.*, J. Colloid Interface Sci. **272**, 444 (2004).
[36] J. L. Dickson *et al.*, Langmuir **19**, 4895 (2003).
[37] S.-Y. Lin and H.-F. Hwang, Langmuir **10**, 4703 (1994).
[38] J. Pich, S. K. Friedlander, and F. S. Lai, J. Aerosol Sci. **1**, 115 (1970).
[39] M. Avrami, J. Chem. Phys. **7**, 1103 (1939).
[40] R. A. Sigsbee, in *Nucleation*, edited by A. C. Zettlemoyer (Marcel Dekker, New York, 1969), p. 151.
[41] V. Talanquer and D. W. Oxtoby, J. Chem. Phys. **104**, 1483 (1996).
[42] J. Ahmad and R. S. Hansen, J. Colloid Interface Sci. **38**, 601 (1972).
[43] H. Reiss, J. Chem. Phys. **19**, 482 (1951).